JCI The Journal of Clinical Investigation

CNS myeloid cells critically regulate heat hyperalgesia

Stefanie Kälin, … , Christian Witzel, Frank L. Heppner

J Clin Invest. 2018. https://doi.org/10.1172/JCI95305.

Research Article In-Press Preview **Neuroscience**

Activation of non-neuronal microglia is thought to play a causal role in spinal processing of neuropathic pain. To specifically investigate microglia-mediated effects in a model of neuropathic pain and overcome methodological limitations of previous approaches exploring microglia function upon nerve injury, we selectively ablated resident microglia by intracerebroventricular (icv) ganciclovir infusion into male *CD11b-HSVTK* transgenic mice, which was followed by a rapid, complete and persistent (23 weeks) repopulation of the CNS by peripheral myeloid cells. In repopulated mice that underwent sciatic nerve injury, we observed a normal response to mechanical stimuli, but an absence of thermal hypersensitivity ipsilateral to the injured nerve. Furthermore, we found that neuronal expression of calcitonin gene-related peptide (CGRP), which is a marker of neurons essential for heat responses, was diminished in the dorsal horn of the spinal cord in repopulated mice. These findings demonstrate distinct mechanisms for heat and mechanical hypersensitivity, highlighting a crucial contribution of CNS myeloid cells in the facilitation of noxious heat.

CNS myeloid cells critically regulate heat hyperalgesia

Stefanie Kälin[1,6], Kelly R. Miller[1,6], Roland E. Kälin[1], Marina Jendrach[1], Christian Witzel[2] & Frank L. Heppner[1,3,4,5]

[1]Department of Neuropathology, Charité - Universitätsmedizin Berlin, ~~Charitéplatz 1, 10117 Berlin, Germany~~

[2]Department of Plastic Surgery, Charité - Universitätsmedizin Berlin, ~~Charitéplatz 1, 10117 Berlin, Germany~~

[3]Cluster of Excellence, NeuroCure, Charitéplatz 1, 10117 Berlin, Germany

[4]Berlin Institute of Health (BIH), Berlin, Germany

[5]German Center for Neurodegenerative Diseases (DZNE) Berlin, 10117 Berlin, Germany

[6]These authors contributed equally to this work

present address S.K.: apceth Biopharma GmbH, Munich, Germany

present address K.R.M.: NanoString Technologies, Seattle, WA 98109, USA

present address R.K.: Neurosurgical Research, University Clinics Munich, Ludwig-Maximilians-University, 81377 Munich, Germany

Address correspondence to: Frank L. Heppner, Department of Neuropathology, Charitéplatz 1, D-10117 Berlin, Tel.: +49 30 450 536042, Fax: +49 30 450 536940, frank.heppner@charite.de

The authors have declared that no conflict of interest exists.

ABSTRACT

Activation of non-neuronal microglia is thought to play a causal role in spinal processing of neuropathic pain. To specifically investigate microglia-mediated effects in a model of neuropathic pain and overcome methodological limitations of previous approaches exploring microglia function upon nerve injury, we selectively ablated resident microglia by intracerebroventricular (icv) ganciclovir infusion into male *CD11b-HSVTK* transgenic mice, which was followed by a rapid, complete and persistent (23 weeks) repopulation of the CNS by peripheral myeloid cells. In repopulated mice that underwent sciatic nerve injury, we observed a normal response to mechanical stimuli, but an absence of thermal hypersensitivity ipsilateral to the injured nerve. Furthermore, we found that neuronal expression of calcitonin gene-related peptide (CGRP), which is a marker of neurons essential for heat responses, was diminished in the dorsal horn of the spinal cord in repopulated mice. These findings demonstrate distinct mechanisms for heat and mechanical hypersensitivity, highlighting a crucial contribution of CNS myeloid cells in the facilitation of noxious heat.

INTRODUCTION

Neuropathic pain refers to a complex chronic pain state resulting from damage to or dysfunction of the somatosensory system that is characterized by mechanical allodynia, hyperalgesia and spontaneous pain in human patients. There is accumulating evidence that neurons are not the only crucial players in spinal processing of nociceptive signals, but that glial cells also contribute to experimental pain states. In particular, microglia, the resident immune cells in the CNS, are powerful modulators in the induction of nociception (1, 2). As a consequence of peripheral nerve injury, microglia in the dorsal horn (DH) of the spinal cord rapidly respond to injury by migrating to the site of damage, proliferating, upregulating a variety of cell-surface receptors and elaborating an array of cytokines. The latter can be causal for the hyperactivity of nociceptive neurons. In addition to the activation of CNS-resident microglia, peripheral axonal injury also results in the recruitment of hematogenous monocytes to the DH, where they also provide a rich source of pain mediators that act on nociceptive terminals (3).

The necessity of microglia and peripheral blood-borne myeloid cells for the initiation of neuropathic pain processing after peripheral nerve injury has not been independently investigated to date due to the lack of appropriate tools to address this question. Thus, we took advantage of a transgenic mouse model that allows for a large-scale depletion of microglia in the CNS, namely, a mouse expressing the CD11b-promoter driven herpes simplex virus thymidine kinase (*CD11b-HSVTK*, referred to hereafter as TK mice) (4, 5). Following microglia ablation in this model, peripheral monocytic cells rapidly infiltrate and repopulate the brain parenchyma (6), thus allowing for the effective exchange of endogenous microglia with peripheral myeloid cells (7). Using the *CD11b-HSVTK* (TK) mouse model, we found that following partial sciatic nerve ligation (PSNL), mice lacking central microglia that are replaced with peripheral myeloid cells fail to develop heat hypersensitivity, but maintain normal responses to mechanical and cold stimulation. In line with this finding, we observed a significant reduction in CGRP, a molecular

marker of peptidergic nociceptive neurons that were shown to be required to sense heat (8). Taken together, we report for the first time on an animal model allowing rapid recruitment of peripheral myeloid cells into the spinal cord parenchyma after depletion of resident microglia. In this way, we were able to experimentally show that the origin of myeloid cells, at least to some extent, determines their functional repertoire demonstrating that the role of resident microglia in neuropathic pain is distinct from that of peripheral myeloid cells and extends beyond acute pro-inflammatory responses that promote the development of pain, but also encompasses the mediation of distinct pain entities.

RESULTS

Myeloid cell response to peripheral nerve injury

Microglial activation can be consistently observed in a variety of experimental peripheral nerve injury models (1, 9). Induction of glial cytokine expression is aligned with morphological changes and increased expression of the myeloid cell-specific marker Iba1 (10). To gain a better understanding of the temporal activation pattern of microglia after PSNL in wild type (WT) mice, Iba1 immunoreactivity (IR) was analyzed in the ipsilateral and contralateral dorsal horn (DHi/DHc) of the lumbar spinal cord at several time points after PSNL. Compared to the contralateral side, microglia surrounding the injured sensory and motor neurons of the sciatic nerve terminals in the ipsilateral dorsal and ventral horn (VH) displayed intense IR (Figure 1A). In the DHi, quantitative morphometric analysis of the area covered by $Iba1^+$ cells demonstrated a substantial increase starting 2 days post injury (dpi), peaking at 7 dpi and declining thereafter (Figure 1B).

Proliferation of microglia was assessed by BrdU incorporation at multiple time points after injury. Compared to naïve lumbar spinal cords in which only few sparse BrdU-immunolabeled cells could be found within the spinal cord parenchyma, vast numbers of newly dividing $BrdU^+$ cells were detected within the DHi from days 2 to 4 after injury (Figure 1, C and D). Double-immunofluorescent staining of incorporated BrdU and Iba1 (Figure 1F) revealed that 94% of $BrdU^+$ cells in the DHi were $Iba1^+$ (Figure 1E).

To unequivocally distinguish blood-derived myeloid cells from intrinsic microglia, we generated chimeric mice harboring isogenic β-actin-GFP-labeled WT bone marrow. Double immunolabeling revealed a clear co-localization of GFP and Iba1 (Figure 1G), confirming that in addition to resident microglia, peripheral myeloid cells also contribute a minor amount to the $Iba1^+$ cell population within the lumbar spinal cord in the early activation phase after PSNL.

Depletion of microglia and persistent repopulation with peripheral myeloid cells in the lumbar spinal cord

Circulating monocytes do not substantially enter or engraft the CNS of healthy mice (11); however, specific pathological conditions, such as peripheral nerve injury, trigger their infiltration (3, 12). To investigate whether behavioral differences in the facilitation of pain signals exist between CNS resident microglia and peripheral myeloid cells, we took advantage of the TK transgenic mouse model, which allows for the central depletion of endogenous $CD11b^+$ microglia in the brain parenchyma followed by rapid repopulation of peripheral myeloid cells upon icv administration of the drug ganciclovir (GCV) (6, 7). However, prior to this study, it remained unclear if other parts of the CNS, namely the lumbar spinal cord, can also be repopulated with peripheral myeloid cells and if they can functionally replace CNS-resident microglia. Thus, a specific exchange protocol for the spinal cord was established that takes advantage of the rapid transport of GCV via the cerebrospinal fluid (CSF) to the lumbar spinal cord. To restrict GCV sensitivity to resident microglia and distinguish between remaining microglia and peripheral myeloid cells after CNS repopulation, we generated GFP bone-marrow chimeric mice that only express the TK transgene in the radioresistant CNS (GFP>TK), as well as non-transgenic WT littermates (GFP>WT).

To circumvent potential side effects of high CCL2 expression, which has been reported to be produced upon irradiation and involved in the recruitment of CCR2-expressing myeloid cell into the CNS (13), we waited for 8 weeks after irradiation and reconstitution with GFP bone marrow before further manipulations were performed (12). Two weeks after initiation of GCV treatment, quantitative stereological analysis revealed that 75% of the myeloid cell pool in the lumbar spinal cord of GFP>TK animals was comprised of GFP^+ peripherally-derived cells (Figure 2B). GFP>TK mice that were analyzed 7 weeks (short term) after termination of GCV treatment exhibited a 92% repopulation (Figure 2, A and C). For all time points tested, GCV-treated

GFP>WT mice (Figure 2, B and C), vehicle-treated (artificial CSF, aCSF; Figure 2D), as well as non-treated GFP>WT and GFP>TK mice (Figure 2E), showed little to no infiltration of GFP^+ myeloid cells into the lumbar spinal cord, indicating that irradiation, reconstitution and GCV administration *per se* did not promote substantial invasion of peripheral myeloid cells. Notably, the number of $Iba1^+$ (and GFP^+) cells increased over time in spinal cord tissue of GCV-treated GFP>TK mice to a similar extent as observed in repopulated brain regions (6, 7).

Interestingly, we observed long-term residency of peripherally-derived GFP^+ myeloid cells in the lumbar spinal cord even half a year after microglia depletion. Specifically, GFP>TK mice that were analyzed 23 weeks (long term) after termination of GCV treatment exhibited a 83% repopulation (Figure 3A). Moreover, analysis of the mean distance between $Iba1^+$ cells revealed a denser distribution of repopulated cells in GFP>TK mice than resident microglia in the lumbar spinal cord of GFP>WT animals (Figure 3, B and C).

Taken together, peripheral myeloid cell repopulation is dependent upon microglia depletion in GFP>TK mice. Compared to resident microglia, infiltrating myeloid cells were more numerous throughout the spinal cord, as expected since they are tasked with covering the same surveillance area as microglia, but lack the elaborate branched processes possessed by CNS-resident microglia.

Long-term myeloid cell accumulation and activation in the DHi after PSNL in repopulated GFP>TK mice

We observed reactive microgliosis at early time points (7 dpi) after PSNL in WT (Figure 1A), GFP>WT, and GFP>TK mice (Figure 4A). To compare the activation kinetics of engrafted myeloid cells with that of resident microglia, we performed immunohistological analyses of the DH of non-repopulated GFP>WT and repopulated GFP>TK animals at late time points (50 dpi) after PSNL. No myeloid cell accumulation and little infiltration of GFP^+ peripheral cells could be

found in the uninjured (contra) and injured (ipsi) DH of GCV-treated GFP>WT animals (Figure 4, G and H) and non-treated (Figure 4B) or aCSF-treated GFP>WT and GFP>TK animals (Figure 4C) at any time point examined. As expected, repopulated GFP>TK sham-operated animals showed no signs of myeloid cell accumulation (Figure 4, D and E). Instead, we identified a robust accumulation of $Iba1^{+}/GFP^{+}$ myeloid cells that were still hypertrophic (Figure 4F), indicating an enhanced response state, at 50 dpi in the DHi of GFP>TK animals, as compared to WT animals at 7 dpi. This observation was made in two independent experiments, namely in the short term group (Figure 4, G and H) in which PSNL was performed two weeks after depletion/repopulation took place, and in the long term group (Figure 4, I and J) in which there was a period of four months between the time of GCV administration (and microglia depletion/myeloid cell repopulation) and PSNL, thus allowing the invading peripheral myeloid cells to adapt to the CNS environment.

Taken together, in contrast to resident microglia in WT and GFP>WT mice, which returned to a homeostatic state one week post-PSNL, infiltrating myeloid cells continued to exhibit a specific reactive phenotype in response to PSNL after 50 dpi, suggesting a differential response of endogenous microglia and peripherally-derived CNS myeloid cells to PSNL at late time points.

Microglia-depleted and myeloid cell repopulated mice lack heat hyperalgesia, but react normally to mechanical and cold stimuli in response to PSNL

Injury to a peripheral nerve produces profound behavioral indicators of persistent pain, including hyperalgesia and allodynia (14). In WT mice, PSNL had no influence on motor function and reflexes, as assessed by the accelerating Rota Rod assay and the Tail Flick test, respectively; however, it produced classic neuropathic pain symptoms, including a decrease in thermal and mechanical paw withdrawal thresholds (PWT) ipsilateral to the injury (Figure S1).

To specifically test whether peripheral myeloid cells are able to functionally replace microglia, we performed PSNL (or sham operation) two weeks after continuous GCV treatment. At that time, the lumbar spinal cord was already repopulated by peripherally-derived GFP^+ cells (Figure 2B). To determine if behavioral responses to heat, cold and mechanical stimuli were affected by the lack of endogenous microglia and presence of peripherally-derived myeloid cells, mice were subjected to the Plantar, incremental Cold Plate and von Frey test, respectively. For all experiments, although GCV administration was stopped prior to PSNL, we assessed GCV- or aCSF-treated GFP>WT and GFP>TK mice before and after GCV/aCSF administration to exclude non-specific effects of surgical procedures and prior GCV treatment. Untreated GFP>WT and GFP>TK animals exhibited similar baseline thresholds to mechanical and thermal stimuli. In all groups tested, GCV-treatment did not produce any baseline changes in PWTs in any of the behavioral tests (Figure 5, A - E), indicating that irradiation, reconstitution and microglia depletion/myeloid cell repopulation had no effect on behavioral responses. Furthermore, motor function (Figure 5A) and reflexes (Figure 5B) were not altered before or after PSNL in any of the tested groups.

In contrast, following PSNL, mechanical allodynia and heat hyperalgesia were observed in GCV-treated GFP>WT and aCSF-treated GFP>WT and GFP>TK control animals. Sham-operated, repopulated GFP>TK mice developed no behavioral hyperalgesia (Figure 5, C and D). Surprisingly however, in GCV-treated GFP>TK mice in which CNS-resident microglia were depleted and had been replaced by peripherally-derived myeloid cells, PSNL resulted in a lasting formation of mechanical allodynia (Figure 5C), while heat withdrawal latencies for the injured paw were identical to that of the uninjured contralateral side (Figure 5D), indicating a complete lack of heat hyperalgesia in repopulated mice. To determine if this phenotype is specific for heat we also measured cold sensitivity in GFP>WT and GFP>TK mice. GFP>WT and GFP>TK mice displayed a greater sensitivity to cold after PSNL (Figure 5E), suggesting that microglia ablation and myeloid cell repopulation had no effect on cold hyperalgesia. Similar

analyses in animals that received PSNL four months after GCV treatment and microglia depletion/engraftment of peripheral myeloid cells (long term) confirmed this observation as these mice also failed to manifest heat hyperalgesia (Figure 5I), but displayed normal mechanical responses (Figure 5H). On the other hand, long term GFP>WT control mice exhibited expected mechanical and heat hyperalgesia (Figure 5, H and I). Again, neither group displayed alterations in the Rota Rod or Tail Flick test (Figure 5, F and G).

Collectively, in chronic pain tests, GFP>TK animals depleted of central microglia and populated by bone-marrow-derived myeloid cells showed considerably decreased PWTs in response to mechanical and cold, but not heat stimuli ipsilateral to the injury.

Microglia depletion and myeloid cell repopulation does not influence established chronic pain symptoms

To test whether ablation of microglia and subsequent repopulation with peripheral myeloid cells can rescue thermal hyperalgesia that occurs after peripheral nerve injury, GCV was administered at 7 dpi, a time point at which robust thermal hyperalgesia and mechanical allodynia were already established (Figure 6 and Figure S1). In contrast to our observations in previous experiments, initiation of microglia depletion and myeloid cell repopulation within the lumbar spinal cord of GCV-treated GFP>TK mice post PSNL did not result in any difference in mechanical or thermal thresholds compared to non-depleted and non-repopulated GFP>WT nerve-injured mice (Figure 6, C and D). No deficits in the Rota Rod (Figure 6A) or Tail flick test (Figure 6B) could be observed in these mice.

This observation suggests that the influence of microglia and/or peripheral macrophages on thermal hyperalgesia, or the lack thereof as observed in the presence of peripheral myeloid cells, results from a lack of initiation at acute stages, rather than an inhibition of maintenance of hyperalgesia.

CGRP expression is reduced in the dorsal horn of microglia-depleted mice

Increased excitatory synaptic transmission and decreased inhibitory synaptic transmission in the DH of the spinal cord are the two most important characteristics for the development of central sensitization (15, 16). To compare the transcription pattern of resident microglia and infiltrating myeloid cells, a qPCR-based microarray (Mouse Pain: Neuropathic & Inflammatory) of all cell populations within the DH of microglia-depleted and myeloid cell-repopulated mice and identically-treated controls was performed 7 dpi. Gene expression analysis led to the identification of a number of presumably microglia-/macrophage-specific inflammatory markers that were significantly upregulated in repopulated GFP>TK mice (Table S1). Yet, none of these target genes were found to be specifically regulated in the DHi compared to DHc, pointing towards a general inflammatory signature of bone marrow-derived myeloid cells repopulating the CNS after microglia depletion, rather than a specific response to PSNL.

Importantly however, we found that *Calca*, encoding the neuron-specific CGRPα protein that was shown to directly contribute to heat sensation (8, 17), was the single gene whose mRNA expression was significantly downregulated in the DH of the spinal cord in GFP>TK mice 7 dpi (Table S1 and Figure 7A), while other neuronal transcripts e.g. *Cacna1b*, *Ntrk1* and *Grin1* were unchanged (data not shown). To determine if this change was detectable at the protein level, we also investigated CGRP-IR in the DH of GFP>WT and GFP>TK animals by morphometric analysis. Independent of PSNL, we found a significantly lower expression of CGRP in microglia-depleted and myeloid cell repopulated mice (Figure 7, B and C). Importantly, there was no reduction in the total neuronal population (Figure 7D), excluding the possibility that a loss of DH neurons causes the decrease in CGRP expression. To directly assess whether changes in neuronal CGRP expression can, in principle, be mediated by myeloid cells, we treated dorsal root ganglia (DRG) F11 cells with conditioned media from ATP- and substance P-stimulated

microglia and peritoneal macrophages and measured the neuronal CGRP release. In line with our *in vivo* observations, we noticed a significant decrease in CGRP levels when neurons were subjected to conditioned media from myeloid cells (Figure 7E).

DISCUSSION

As described for other models of neuropathic pain, we observed an activation of myeloid cells including both resident microglia and peripherally derived myeloid cells, which responded to the nerve injury in a temporally and spatially restricted fashion within the lumbar spinal cord, indicating that resident microglia and/or peripheral myeloid cells can influence the initiation of persistent pain in WT mice (1, 2, 12, 18). Previous findings point to an involvement of myeloid cells in the initiation of exaggerated pain responses, such as attenuated mechanical allodynia in rats after spinal nerve transection upon non-selective inhibition of spinal cord myeloid cells by minocycline (19). In addition, mice deficient in the chemokine receptor CCR2 or the fractalkine receptor CX3CR1 failed to develop mechanical allodynia and/or thermal hyperalgesia after PSNL (20, 21), while mice with a microglia-specific lack of brain-derived neurotrophic factor (BDNF) failed to develop morphine-induced hyperalgesia (22). These findings support the hypothesis that myeloid cells modulate neuronal activity in the spinal cord following peripheral nerve injury. However, methodological limitations of the approaches utilized thus far left many unanswered questions. For example, minocycline, besides conferring numerous divergent effects apart from being antinflammatory (23, 24), has been shown to be insufficient in preventing aspects of microglia activation, particularly after nerve injury (25). Furthermore, genetic deletion of microglia-specific receptors/signaling pathways may lead to abnormal compensatory changes in mutant microglia, thus confounding data interpretation. Therefore, we set out to dissect the precise role of resident microglia by utilizing male *CD11b-HSVTK* transgenic mice (4) to specifically and entirely deplete these cells in a neuropathic pain setting. Male animals were used to avoid confounders, such as timing of ovulation.

Unlike other microglia depletion models in which ablated microglia are replaced CNS-intrinsically through proliferation of endogenous microglia (26), depletion of microglia in TK mice has been shown to induce rapid recruitment of peripheral myeloid cells into the brain parenchyma upon icv administration of GCV (6, 7), making this model uniquely suited to study differential effects of

microglia and peripheral myeloid cells in the brain. Thus, TK mice differ from other published microglia depletion models since in the latter, microglia are replaced by proliferating cells within the CNS, most likely due to a difference in the molecular mechanism of depletion (26, 27). Therefore, we examined neuropathic pain and related mechanisms in the absence of resident microglia and presence of peripheral myeloid cells to identify shared myeloid contributions to the neuropathic pain phenotype and uncover behavioral distinctions between CNS-resident and peripheral myeloid cells in this setting.

Surprisingly, infiltrating myeloid cells exhibited activation in the DHi up to 50 days after PSNL when activation of resident microglial has usually subsided, suggesting a differential response of endogenous microglia and peripherally-derived CNS myeloid cells to PSNL at late time points. Moreover, microglia-depleted GFP>TK animals harboring peripherally-derived myeloid cells displayed considerably decreased PWTs in response to mechanical or cold, but not to heat stimuli ipsilateral to PSNL at all time points tested, indicating a selective role of microglia in the etiology of PSNL-induced heat sensitivity, while in other pain modalities - namely mechanical or cold sensation - peripheral myeloid cells were able to take over functions of local microglia. However, mechanistically, we cannot rule out that the observed lack of heat hyperalgesia is a consequence of pain-modulating mediators that are released by the high numbers of infiltrating peripheral myeloid cells, conversely implicating peripheral myeloid cells as unique modulators of pain. That microglia depletion and myeloid cell repopulation does not influence established chronic pain symptoms is in line with the theory that microglia are involved in early and acute responses to nerve injury, but not for the sustainment of neuropathic pain symptoms, while astrocytes are the main players in the maintenance of neuropathic pain, but not critically involved in its development (28, 29). Microglia have been shown to participate in central sensitization by modulation of synaptic transmission and amplification of pro-nociceptive signals, for example via the release of TNFα, IL-6, and BDNF in the DH of the spinal cord (30, 31). When we examined the transcription pattern of resident microglia and engrafted myeloid cells, none of

the above-mentioned genes were differentially expressed between GFP>WT and GFP>TK mice. However, we identified a number of presumably microglia-/macrophage-specific inflammatory markers that were significantly upregulated in repopulated GFP>TK mice, e.g. *Ccl12* and *Ccr2*. Since the identified genes were specific to the condition of microglia depletion and myeloid cell repopulation, but not related to the PSNL, they appear to regulate the process of chemokine-mediated recruitment of peripheral myeloid cells to the CNS. This is in line with recent studies in the field demonstrating that indeed, microglia do express a genetic profile distinct from peripheral myeloid cells (32-34).

When further dissecting the molecular underpinnings of how resident microglia specifically and distinctively mediate thermal hyperalgesia, we only found *Calca* (the gene encoding CGRPα), among 84 genes, to be significantly downregulated in the DH of the lumbar spinal cord of GFP>TK mice. While our *in vitro* experiment further supports the notion that myeloid cells act as critical regulators of CGRP expression or survival of CGRP-expressing somatosensory neurons, it does not suffice to distinguish defined *in vivo* functions of resident microglia from those of peripheral myeloid cells, since myeloid cells *in vitro* are known to adapt myriad phenotypes (32, 35) contrasting the *in vivo* setting, in which the CNS microenvironment orchestrates and confines microglia phenotypes. For this reason, the herein described experimental *in vivo* setting was necessary to reliably address the question of whether myeloid cells of various origins indeed execute distinct functions independent from their microenvironment.

Notably, heat hyperalgesia, in particular, is mediated by antinociceptive CGRP expression (17). Importantly, CGRP-IR of DRG neurons was shown to directly contribute to noxious heat sensation, while mechanosensation was unaffected in CGRPα–DTR$^{+/-}$ mice (8), thus providing an explanation for the herein described phenotype of GFP>TK animals. While we found diminished CGRP expression on both the injured and uninjured sides of the spinal DH (as a consequence of the repopulation process and not the PSNL), we did not detect increased heat withdrawal latencies in the contralateral paw. This suggests that a broader loss of CGRPα-

lineage neurons is required for a complete lack of heat sensitivity in the uninjured paw (8), whereas a mild reduction in CGRP expression appears to be sufficient to result in a loss of heat hypersensitivity under pathological conditions, such as PSNL, thus introducing a novel, non-neuronal approach to manipulate pathological pain. Because homeostatic and activated microglia also interact with and thereby shape the connectivity and function of the tripartite synapse in the healthy CNS (36-38), compromised synaptic transmission by $CGRP^+$ primary sensory neurons is conceivable in the microglia-depleted/myeloid cell repopulated setting given the close proximity of activated microglia and peripheral myeloid cells with the central terminal zone of the injured afferents (39-41). However, we did not detect differential expression of *Calca* or CGRP-IR within DRG between GFP>WT and GFP>TK mice (data not shown). This might be explained by the fact that icv GCV treatment does not deplete $Iba1^+$ satellite glia outside the CNS, therefore not triggering CGRP reduction. Moreover, CGRP is known to be locally synthesized in the spinal cord e.g. in deeper lamina dorsal horn neurons (42), as well as during axonal regeneration (43), indicating that microglia depletion and/or myeloid cell repopulation in the dorsal horn directly target this local CGRP synthesis via non-contact mediated effects that could be solely responsible or act in conjunction with contact-mediated processes, such as synaptic pruning.

Taken together, our data show that peripheral nerve injury-induced microglia activation in the DH of the spinal cord plays a critical and unique regulatory role serving to modulate activity of CGRPα primary sensory neurons, a function that infiltrating myeloid cells cannot necessarily incur. Importantly, the overall physiological potential of these two cell populations, namely resident microglia and peripherally-derived myeloid cells, can be considered both distinct and redundant depending on the pain entity. Experimental approaches in similar preclinical animal models involving introduction of genetically engineered myeloid cells to the CNS following depletion of resident microglia upon PSNL may serve to elucidate the molecular underpinnings of microglia-neuronal cross-talk in the context of neuropathic pain. This knowledge may

ultimately allow for the direct modification of CNS myeloid cell actions to modulate pathologic pain responses resulting in novel, targeted cell-based therapeutic intervention.

METHODS

Animals. All experiments were conducted with adult (150-200 days old) male hemizygous *CD11b-HSVTK* (TK) mice (4) or transgene negative littermates (referred to as wild-type, WT), which were originally derived on a B6D2 background and were backcrossed to C57BL/6 mice for more than 12 generations. Mice were kept under pathogen-free, temperature- and humidity-controlled conditions, on a 12/12 h light/dark cycle, with access to food and water *ad libitum*. Data from all animals were included for all respective analyses unless an animal had to be excluded due to death prior to finalizing the study.

In vivo manipulations. Bone marrow chimeric mice were generated as described previously (5). Briefly, recipient mice were exposed to 10 Gy whole-body irradiation, after which they received intravenous injection of $1x10^7$ bone marrow cells obtained from tibia and femur of B6-Tg(ACTbEGFP)1Osb mice (Jackson Laboratories). Subsequently, mice received treatment with antibiotics (0.01% Enrofloxacin, Baytril®, Bayer Vital) for one month. Animals were subjected to PSNL 10 weeks (short term) or 6 months (long term) after transplantation. For icv GCV (8 mg/ml Cymevene®, Roche) application, implantation of miniosmotic pumps (Model 2002, 0.5 µl/h; Alzet®) was performed as previously described (5). After 4 weeks, the pump reservoir was removed without disturbing the brain infusion cannula. Table 1 depicts the various experimental groups.

Peripheral nerve injury. Partial sciatic nerve ligation (PSNL) was conducted under Ketamine/Xylazine (Ketamine 100 mg/kg, Xylazine 10 mg/kg) anesthesia. The right sciatic nerve was exposed at high-thigh level and the dorsal 1/2 to 1/3 diameter of the common sciatic nerve was tightly ligated with 10/0 silk (Prolene™, Ethicon). In sham-operated animals the nerve was exposed as in the PSNL procedure, but not ligated.

Antibodies. Rabbit anti-Iba1 (Wako Chemicals, 019-19741, 1:500 dilution), rabbit anti-GFP (Abcam, ab290, 1:1000 dilution), rat anti-BrdU (AbD Serotec, OBT0030G, 1:500 dilution), mouse anti-NeuN (Millipore, MAB377, 1:500 dilution) and rabbit anti-CGRP (Enzo Life Sciences, CA1137, 1:200 dilution) were used.

Histology and confocal microscopy. Animals were perfused with isotonic NaCl (0.9%) solution followed by 4% paraformaldehyde (PFA) under deep Ketamine/Xylazine anesthesia (Ketamine 100 mg/kg; Xylazine 10 mg/kg). Spinal cords were removed and fixed in 4% PFA for two days. Subsequently, L4-L6 segments were removed and immersed in 30% sucrose for at least 24 h at 4 °C. 30 µm thick coronal sections were cut on a cryostat and processed free-floating. Sections were incubated for 1 h at room temperature in PBS containing 0.3% Triton X-100 and 10% normal goat serum (NGS). Primary antibodies were applied and incubated overnight at 4 °C in PBS containing 0.3% Triton X-100 and 5% NGS. After 3 washes in PBS, spinal sections were incubated with secondary antibodies conjugated to Alexa Fluor® or avidin-peroxidase (Dianova, dilution 1:300). For BrdU-labeling, sections were pre-treated with 50% formamide in 2 x standard saline citrate (SSC) for 2 h at 65 °C, followed by 2 x 5 min in 2 x SSC at room temperature, 30 min in 2 N HCl at 37 °C and 10 min in 0.1 M borate buffer prior to immunostaining. Multiple immunofluorescent images were acquired using a Zeiss LSM 5 *Exciter* confocal-laser-scanning system. Images were processed in Photoshop CS3.

Cell counts and quantifications. Morphometric quantification of reactive microglia in WT mice after PSNL was performed using the Cell D analysis system (Olympus, version 5.1). Defined regions containing the DHi and DHc in the L4-L6 spinal cord of 8-10 randomly selected sections per animal (n = 4/time point) stained with Iba1 were analyzed by determining the percentage of area covered of $Iba1^+$ cells, using the color filter and phase analysis tool. The total number of BrdU-labeled cells was quantified in the DHi and DHc in the L4-L6 spinal cord (8-10 sections/animal, n = 4) using a light microscope. For the quantification of double positive BrdU

and Iba1 cells, confocal *z*-stacks were generated to confirm signal co-localization. 2 sections/animal (n = 5) at 2 or 4 dpi were scanned at 20 x magnification for BrdU and Iba1 co-labeled cells. For reconstituted mice, the number of microglia and peripheral derived myeloid cells was stereologically assessed in the lumbar spinal cord on random sets of every 10^{th} systematically sampled 30 µm thick Iba1- and GFP-immunostained section (yielding 10-12 sections/mouse). Analysis was performed with the aid of the StereoInvestigator® software (Microbrightfield, version 10) and a motorized *x-y-z* stage coupled to a video-microscopy system (Olympus BX35F) using the optical fractionator workflow (44). *NeuN quantification:* $NeuN^+$ neuronal cell bodies were quantified throughout the entire DH represented by 12 systematically sampled 30 µm thick free-floating sections per animal. Analyses were performed with the aid of the StereoInvestigator® software (Microbrightfield, version 10) and a motorized *x-y-z* stage coupled to a video-microscopy system (Olympus BX35F) using the meander scan function. *Mean distance:* Measurements of the distance between neighboring cell bodies and cross-sectional areas of $Iba1^+$ microglia (20 distances or cell bodies/section, 5 sections/animal, n > 4/group) were made by using the CellSense (Olympus, version 1.6) analysis system for the mean distance and cell body size analysis, respectively. Morphometric analysis of the immunohistochemical $CGRP^+$ area of icv GCV-treated GFP>WT and GFP>TK mice was performed using the CellSense analysis system (Olympus, version 1.6) in the lumbar DH of 6-7 sections.

Behavioral studies. As a pre-requisite for inclusion for analysis of behavioral data, efficacy of microglia depletion and repopulation (>70%) was confirmed through analysis of the lumbar spinal cord of all GFP>TK mice. Before behavioral testing, mice were acclimated to the testing room, the equipment and the experimenter for one week. To evaluate the effects of microglia depletion on thermal hyperalgesia and mechanical allodynia, motor function and reflexes, mice underwent a comprehensive behavioral test battery before surgery and at 4, 8, 12 and 14 post-icv treatment, as well as at post-nerve injury days (dpi) 3, 7, 14, 21, 35 and 50. Mice were

acclimated to all testing procedures for 10 min each for one week prior to the start of the experiment, for 5 min before each testing session and for 10 min each on a daily basis throughout the entire testing period. *von Frey test:* To assess punctate tactile sensitivity, threshold responses to calibrated retractable von Frey monofilaments (BioSeb), based on the up-down method in rats (45), were measured. Depending on the response of the animal, increasing or decreasing strength of von Frey filaments were applied sequentially to the mid-line of the plantar surface of each hind paw. The stimulus intensity threshold represents the smallest force that repeatedly elicits withdrawal of the hind paw during 9 trials. Together with the force of the final filament, the 50% response threshold was calculated for both ipsilateral and contralateral paws and expressed as ipsilateral/contralateral ratios. *Tail Flick test:* The tails of mice were exposed to a radiant heat source (25%) until tail withdrawal (flicking response) or signs of struggle. A cut-off time of 30 s was imposed to avoid injury to the tail. *Plantar test:* Thermal sensitivity was tested using the Hargreaves` method (46) with a Plantar test apparatus (IITC Life Sciences, Series 8, Model 390). The latency to withdraw the ipsilateral and contralateral hind paw from the light radiant heat source (25%) placed underneath was recorded. Both hind paws were tested twice with at least 5 min in between. To avoid tissue damage, the heat stimulus was removed after 30 s. Means were calculated and expressed as ipsilateral/contralateral ratios. *Dynamic Cold Plate test:* Cold hyperalgesia was assessed on the incremental Cold Plate (IITC Life Sciences, Series 8, Model PE34). A cut-off temperature of 0 °C was imposed to avoid potential tissue damage. Mice were immediately removed from the cold plate after a reaction (paw licking, flinching or shaking) was observed. To avoid cold stress, two test rounds were performed with an interval of one hour. *Rota Rod test:* The Rota Rod test is a standard test for motor function, coordination and balance. After several training sessions (three 10 rpm trials and two 20 rpm trials over two days each), mice were tested on the Rota Rod (TSE Systems, Series 3375), which increased in speed from 4 rpm to 40 rpm in 300 s. The latency to

fall off the rod was measured in two consecutive trials and the mean latency was used for analysis.

RNA extraction. L4-L6 tissue was vertically separated by median and further dissected to DHi and DHc. Tissue pieces were subjected to total RNA extraction using the InviTrap® Spin Tissue RNA Mini Kit (Invitek Inc., Berlin, Germany). Quality and ribosomal RNA band integrity of isolated RNA was assessed by determining the integrity of the 28S and 18S band using the Agilent 6000 Nano Kit (Agilent Technologies) measured with the Bioanalyzer 2100 (Agilent Technologies, Santa Clara, CA, USA) according to the manufacturer's instructions.

Quantitative real-time PCR array. For the PCR array-based analysis of pain-related genes, 200 ng RNA obtained from the DHi and DHc of GFP>WT and GFP>TK mice (n = 4/group) was reverse transcribed using the RT^2 First Strand Kit according to the manufacturer's instructions (SABioscience). RT^2 Profiler PCR Array PAMM-162ZA (SABiosciences) was used for gene expression analysis. All steps were performed according to the manufacturer's protocol for the ABI 7900HT Sequence Detection System. The specificity of amplification was assessed by melting curve evaluation. Web-based analysis of the 84 genes was performed on the company's website (http://www.sabiosciences.com/pcrarraydataanalysis.php). Data were normalized to *Gapdh*.

Complementary DNA synthesis and quantitative real-time PCR. 600 ng RNA was converted to cDNA using the QuantiTect *reverse transcription* kit (Quiagen), according to the manufacturer's protocol. To detect mRNA expression in dorsal horn samples from GFP>WT and GFP>TK animals (n = 4/group), quantitative real-time PCR was performed using on-demand TaqMan® gene expression assays (Life Technologies) for *Calca* (Mm03749347_m1) on the ABI 7900HT Real-Time PCR System. Samples were run in triplicate for each individual condition. The relative expression levels of the target gene were normalized to that of *Gapdh*. Subsequent analysis was performed using the Δ/ΔCt method.

In vitro assay (cell culture, FACS and ELISA). To measure CGRP levels, dorsal root ganglia F11 cells (ECACC 08062601, kindly provided by Dr. Robert Wellhausen, Fraunhofer IZI, Berlin) were treated with conditioned media derived from FACS-sorted microglia or from peritoneal macrophages that were subjected to 5 mM ATP and 6.2 mM substance P for 3 h. After 1 h, the supernatant was removed and stored at -80°C until use. As a control, additional F11 cells were either treated with ATP and substance P or medium only for 1 h. CGRP concentration was determined by a CGRP-ELISA Kit according to the manufacturer's instruction (CEA876Mu, Cloud-Clone Corp., TX, USA). Each sample was run in triplicate and CGRP concentrations were calculated against total protein contents of the samples, which were assessed following the BCA™ Protein Assay instructions (Thermo Scientific, Rockford, IL, USA).

Statistics. Statistical analysis was performed using SPSS software. For pairwise comparisons of experimental groups, the two-tailed student's *t* test was used. To compare means of three or more samples, one-way ANOVA with Bonferroni´s *post hoc* analysis was used. We applied linear mixed models (random intercept), which use all available data of all mice in one model for each outcome separately in figure 5. In these models the specific outcome was the dependent variable, while dummy codes for the group (GROUP) and the time range after the surgery (SURGERY coded 1 for all time points after surgery and 0 before) as well as a covariate for time (TIME) (in days over the whole study period) were the independent variables. We additionally included interaction terms for GROUP*SURGERY, TIME*SURGERY, and TIME*GROUP to account for differential changes in the groups. In *post hoc* tests we tested group differences at 14 and 50 dpi. Adjustment for multiple testing was done within each model using Bonferroni correction. Results were expressed as mean values ± standard errors of the mean (SEM). Significance was considered as follows: *$p < 0.05$, **$p < 0.01$, and ***$p < 0.001$. ~~In Figure 5, significance is depicted only for the last time point tested.~~

Study approval. All protocols were reviewed and approved by an appropriate institutional review board (regional offices for health and social services, Berlin).

AUTHOR CONTRIBUTIONS

K.R.M. and F.L.H. designed the experiments. S.K., R.E.K. and C.W. conducted the experiments. S.K. and K.R.M. wrote the manuscript, supervised and edited by F.L.H.

ACKNOWLEDGMENTS

We thank Prof. Matthias Endres and Prof. York Winter for allowing us to perform the behavioral tests in their units, Dr. Gerit Pfuhl for introducing the tests to us, Alexander Haake for neuronal quantifications, Claudia Hempt and Sara Mirali for quantifying microglial mean distances and cell bodies, Dr. Robert Wellhausen for providing F11 cells, and Dr. Ulrike Grittner for biostatistical support in applying the linear mixed models. This work was supported by the Deutsche Forschungsgemeinschaft (SFB TRR 43, SFB TRR 167, NeuroCure Exc 257 and HE 3130/6-1 to FLH), by the Berlin Institute of Health (BIH; Collaborative Research Grant to FLH), by the German Center for Neurodegenerative Diseases (DZNE) Berlin, and by a fellowship of ZIBI-IMPRS Graduate School to SK. The authors declare no competing financial interests.

REFERENCES

1. Zhang J, and De Koninck Y. Spatial and temporal relationship between monocyte chemoattractant protein-1 expression and spinal glial activation following peripheral nerve injury. *Journal of neurochemistry.* 2006;97(3):772-83.
2. Milligan ED, and Watkins LR. Pathological and protective roles of glia in chronic pain. *Nature reviews Neuroscience.* 2009;10(1):23-36.
3. Echeverry S, Shi XQ, Rivest S, and Zhang J. Peripheral nerve injury alters blood-spinal cord barrier functional and molecular integrity through a selective inflammatory pathway. *The Journal of neuroscience : the official journal of the Society for Neuroscience.* 2011;31(30):10819-28.
4. Heppner FL, Greter M, Marino D, Falsig J, Raivich G, Hovelmeyer N, et al. Experimental autoimmune encephalomyelitis repressed by microglial paralysis. *Nat Med.* 2005;11(2):146-52.
5. Grathwohl SA, Kalin RE, Bolmont T, Prokop S, Winkelmann G, Kaeser SA, et al. Formation and maintenance of Alzheimer's disease beta-amyloid plaques in the absence of microglia. *Nature neuroscience.* 2009;12(11):1361-3.
6. Varvel NH, Grathwohl SA, Baumann F, Liebig C, Bosch A, Brawek B, et al. Microglial repopulation model reveals a robust homeostatic process for replacing CNS myeloid cells. *Proceedings of the National Academy of Sciences of the United States of America.* 2012;109(44):18150-5.
7. Prokop S, Miller KR, Drost N, Handrick S, Mathur V, Luo J, et al. Impact of peripheral myeloid cells on amyloid-beta pathology in Alzheimer's disease-like mice. *The Journal of experimental medicine.* 2015;212(11):1811-8.
8. McCoy ES, Taylor-Blake B, Street SE, Pribisko AL, Zheng J, and Zylka MJ. Peptidergic CGRPalpha primary sensory neurons encode heat and itch and tonically suppress sensitivity to cold. *Neuron.* 2013;78(1):138-51.

9. Colburn RW, Rickman AJ, and DeLeo JA. The effect of site and type of nerve injury on spinal glial activation and neuropathic pain behavior. *Exp Neurol.* 1999;157(2):289-304.
10. Kettenmann H, Hanisch UK, Noda M, and Verkhratsky A. Physiology of microglia. *Physiological reviews.* 2011;91(2):461-553.
11. Ginhoux F, Greter M, Leboeuf M, Nandi S, See P, Gokhan S, et al. Fate mapping analysis reveals that adult microglia derive from primitive macrophages. *Science.* 2010;330(6005):841-5.
12. Zhang J, Shi XQ, Echeverry S, Mogil JS, De Koninck Y, and Rivest S. Expression of CCR2 in both resident and bone marrow-derived microglia plays a critical role in neuropathic pain. *The Journal of neuroscience : the official journal of the Society for Neuroscience.* 2007;27(45):12396-406.
13. Mildner A, Schmidt H, Nitsche M, Merkler D, Hanisch UK, Mack M, et al. Microglia in the adult brain arise from Ly-6ChiCCR2+ monocytes only under defined host conditions. *Nature neuroscience.* 2007;10(12):1544-53.
14. Sandkuhler J. Models and mechanisms of hyperalgesia and allodynia. *Physiological reviews.* 2009;89(2):707-58.
15. Woolf CJ. Central sensitization: implications for the diagnosis and treatment of pain. *Pain.* 2011;152(3 Suppl):S2-15.
16. Basbaum AI, Bautista DM, Scherrer G, and Julius D. Cellular and molecular mechanisms of pain. *Cell.* 2009;139(2):267-84.
17. Mogil JS, Miermeister F, Seifert F, Strasburg K, Zimmermann K, Reinold H, et al. Variable sensitivity to noxious heat is mediated by differential expression of the CGRP gene. *Proceedings of the National Academy of Sciences of the United States of America.* 2005;102(36):12938-43.
18. McMahon SB, and Malcangio M. Current challenges in glia-pain biology. *Neuron.* 2009;64(1):46-54.

19. Raghavendra V, Tanga F, and DeLeo JA. Inhibition of microglial activation attenuates the development but not existing hypersensitivity in a rat model of neuropathy. *J Pharmacol Exp Ther.* 2003;306(2):624-30.

20. Abbadie C, Lindia JA, Cumiskey AM, Peterson LB, Mudgett JS, Bayne EK, et al. Impaired neuropathic pain responses in mice lacking the chemokine receptor CCR2. *Proceedings of the National Academy of Sciences of the United States of America.* 2003;100(13):7947-52.

21. Staniland AA, Clark AK, Wodarski R, Sasso O, Maione F, D'Acquisto F, et al. Reduced inflammatory and neuropathic pain and decreased spinal microglial response in fractalkine receptor (CX3CR1) knockout mice. *Journal of neurochemistry.* 2010;114(4):1143-57.

22. Ferrini F, Trang T, Mattioli TA, Laffray S, Del'Guidice T, Lorenzo LE, et al. Morphine hyperalgesia gated through microglia-mediated disruption of neuronal Cl(-) homeostasis. *Nature neuroscience.* 2013;16(2):183-92.

23. Keller AF, Gravel M, and Kriz J. Treatment with minocycline after disease onset alters astrocyte reactivity and increases microgliosis in SOD1 mutant mice. *Exp Neurol.* 2011;228(1):69-79.

24. Yang L, Sugama S, Chirichigno JW, Gregorio J, Lorenzl S, Shin DH, et al. Minocycline enhances MPTP toxicity to dopaminergic neurons. *Journal of neuroscience research.* 2003;74(2):278-85.

25. Fendrick SE, Miller KR, and Streit WJ. Minocycline does not inhibit microglia proliferation or neuronal regeneration in the facial nucleus following crush injury. *Neuroscience letters.* 2005;385(3):220-3.

26. Elmore MR, Najafi AR, Koike MA, Dagher NN, Spangenberg EE, Rice RA, et al. Colony-stimulating factor 1 receptor signaling is necessary for microglia viability, unmasking a microglia progenitor cell in the adult brain. *Neuron.* 2014;82(2):380-97.

27. Bruttger J, Karram K, Wortge S, Regen T, Marini F, Hoppmann N, et al. Genetic Cell Ablation Reveals Clusters of Local Self-Renewing Microglia in the Mammalian Central Nervous System. *Immunity.* 2015;43(1):92-106.

28. Suter MR, Wen YR, Decosterd I, and Ji RR. Do glial cells control pain? *Neuron glia biology.* 2007;3(3):255-68.

29. Vallejo R, Tilley DM, Vogel L, and Benyamin R. The role of glia and the immune system in the development and maintenance of neuropathic pain. *Pain Pract.* 2010;10(3):167-84.

30. Kawasaki Y, Zhang L, Cheng JK, and Ji RR. Cytokine mechanisms of central sensitization: distinct and overlapping role of interleukin-1beta, interleukin-6, and tumor necrosis factor-alpha in regulating synaptic and neuronal activity in the superficial spinal cord. *The Journal of neuroscience : the official journal of the Society for Neuroscience.* 2008;28(20):5189-94.

31. Coull JA, Beggs S, Boudreau D, Boivin D, Tsuda M, Inoue K, et al. BDNF from microglia causes the shift in neuronal anion gradient underlying neuropathic pain. *Nature.* 2005;438(7070):1017-21.

32. Butovsky O, Jedrychowski MP, Moore CS, Cialic R, Lanser AJ, Gabriely G, et al. Identification of a unique TGF-beta-dependent molecular and functional signature in microglia. *Nature neuroscience.* 2014;17(1):131-43.

33. Buttgereit A, Lelios I, Yu X, Vrohlings M, Krakoski NR, Gautier EL, et al. Sall1 is a transcriptional regulator defining microglia identity and function. *Nat Immunol.* 2016;17(12):1397-406.

34. Keren-Shaul H, Spinrad A, Weiner A, Matcovitch-Natan O, Dvir-Szternfeld R, Ulland TK, et al. A Unique Microglia Type Associated with Restricting Development of Alzheimer's Disease. *Cell.* 2017;169(7):1276-90 e17.

35. Ransohoff RM. How neuroinflammation contributes to neurodegeneration. *Science.* 2016;353(6301):777-83.

36. Tremblay ME, Stevens B, Sierra A, Wake H, Bessis A, and Nimmerjahn A. The role of microglia in the healthy brain. *The Journal of neuroscience : the official journal of the Society for Neuroscience.* 2011;31(45):16064-9.

37. Wake H, Moorhouse AJ, Jinno S, Kohsaka S, and Nabekura J. Resting microglia directly monitor the functional state of synapses in vivo and determine the fate of ischemic terminals. *The Journal of neuroscience : the official journal of the Society for Neuroscience.* 2009;29(13):3974-80.

38. Kettenmann H, Kirchhoff F, and Verkhratsky A. Microglia: new roles for the synaptic stripper. *Neuron.* 2013;77(1):10-8.

39. Liu L, Persson JK, Svensson M, and Aldskogius H. Glial cell responses, complement, and clusterin in the central nervous system following dorsal root transection. *Glia.* 1998;23(3):221-38.

40. Winkelstein BA, Rutkowski MD, Sweitzer SM, Pahl JL, and DeLeo JA. Nerve injury proximal or distal to the DRG induces similar spinal glial activation and selective cytokine expression but differential behavioral responses to pharmacologic treatment. *The Journal of comparative neurology.* 2001;439(2):127-39.

41. Tsuda M, Inoue K, and Salter MW. Neuropathic pain and spinal microglia: a big problem from molecules in "small" glia. *Trends in neurosciences.* 2005;28(2):101-7.

42. Tie-Jun SS, Xu Z, and Hokfelt T. The expression of calcitonin gene-related peptide in dorsal horn neurons of the mouse lumbar spinal cord. *Neuroreport.* 2001;12(4):739-43.

43. Toth CC, Willis D, Twiss JL, Walsh S, Martinez JA, Liu WQ, et al. Locally synthesized calcitonin gene-related Peptide has a critical role in peripheral nerve regeneration. *Journal of neuropathology and experimental neurology.* 2009;68(3):326-37.

44. Long JM, Kalehua AN, Muth NJ, Hengemihle JM, Jucker M, Calhoun ME, et al. Stereological estimation of total microglia number in mouse hippocampus. *Journal of neuroscience methods.* 1998;84(1-2):101-8.

45. Chaplan SR, Bach FW, Pogrel JW, Chung JM, and Yaksh TL. Quantitative assessment of tactile allodynia in the rat paw. *Journal of neuroscience methods.* 1994;53(1):55-63.

46. Hargreaves K, Dubner R, Brown F, Flores C, and Joris J. A new and sensitive method for measuring thermal nociception in cutaneous hyperalgesia. *Pain.* 1988;32(1):77-88.

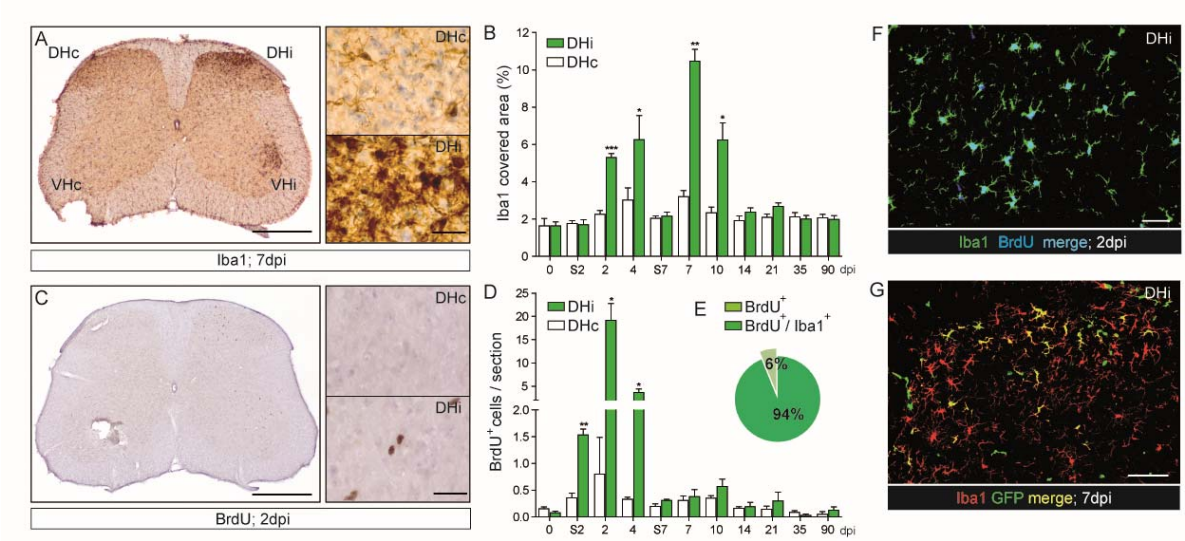

Figure 1. PSNL evokes reactive microgliosis and infiltration of bone marrow-derived myeloid cells into the DHi of WT mice. (A) An increase in Iba1-IR in the lumbar spinal cord of WT animals is seen in the DHi and VHi. Scale bar: 500 µm, Scale bar inset: 25 µm. (B) The temporal profile of Iba1$^+$ microglia activation was determined in the DHi and DHc of the lumbar spinal cord (8-10 sections/mouse, 4 mice/time point, S = sham) and revealed a significant increase in the Iba1-covered area from 2-10 dpi, peaking at 7 dpi. (C) Increased numbers of BrdU$^+$ cells can be detected in the lumbar DHi and VHi. Scale bar: 500 µm, Scale bar inset: 25 µm. (D) Within the DHi, the highest number of BrdU$^+$ cells was found at 2 and 4 dpi (8-10 sections/mouse, 4 mice/time point, S = sham). (E) 94% of total BrdU$^+$ cells were also Iba1$^+$. (F) PSNL-induced proliferation of Iba1 (green) and BrdU (blue) double-positive cells (merge) was restricted to the DHi. Scale bar: 25 µm. (G) Confocal microscopy revealed bone marrow-derived GFP$^+$ cells (green) co-localizing with the myeloid cell marker Iba1 (red) in the DHi of GFP-bone marrow chimeric mice at 7 dpi after PSNL. Scale bar: 50 µm. Error bars represent SEM. Paired two-tailed student´s t-test was performed to compare DHc and DHi for each time point. *$p < 0.05$, **$p < 0.01$, ***$p < 0.001$

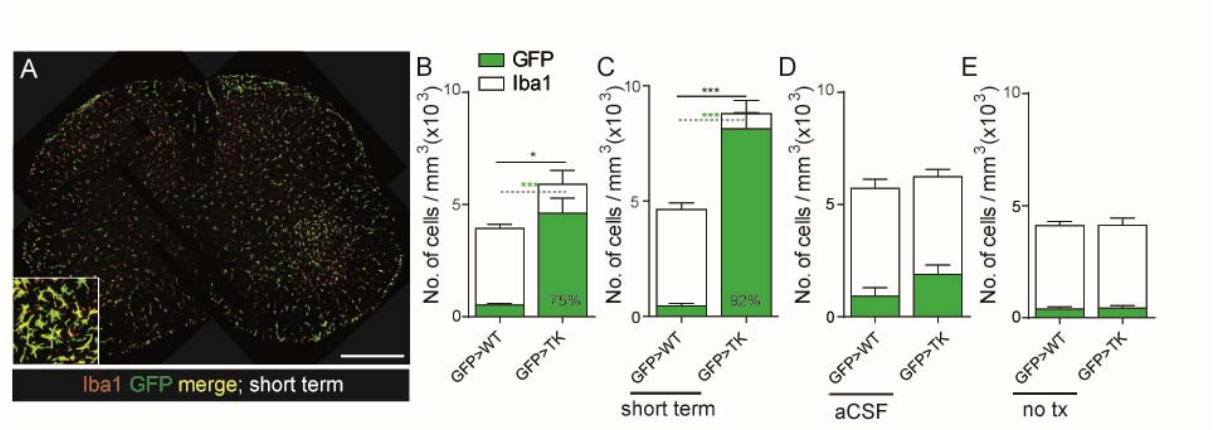

Figure 2. Repopulation in GFP>TK animals. (A) Confocal microscopic analysis of peripherally-derived myeloid cells in the lumbar spinal cord revealed that almost all GFP⁺ cells (green) were also Iba1⁺ (red) after microglia depletion. Merged picture. Scale bar: 500 µm. (B and C) Quantitative stereological analysis of total Iba1⁺ and GFP⁺ cells in the contralateral lumbar spinal cord of GFP>TK mice treated with GCV, either continuously (n = 8) or short term (n = 10), revealed a 75% and 92% repopulation with peripheral myeloid cells, respectively, whereas their corresponding GFP>WT littermates (continuously, n = 10; short term, n = 9) showed an average of only 10% GFP⁺ cells. (D and E) Vehicle (aCSF)-treated (n = 8/genotype), as well as non-treated (no tx) GFP>WT (n = 9) and GFP>TK (n = 4) mice showed only little infiltration of peripheral myeloid cells. Dashed line with green asterisks for comparing GFP⁺ cells. Error bars represent SEM. Paired two-tailed student´s t-test for corresponding GFP>WT and GFP>TK pairs. *p < 0.05, ***p < 0.001

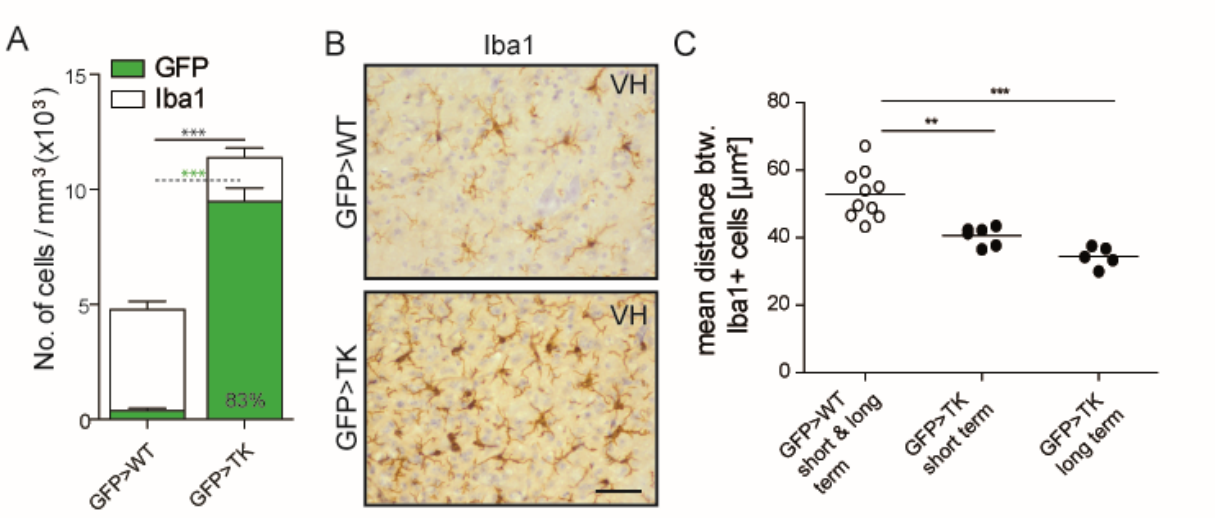

Figure 3. Sustained repopulation in GFP>TK animals. (A) GFP>TK mice (n = 5) showed that 83% of all myeloid cells in the lumbar spinal cord are of peripheral origin (GFP^+) 6 months after terminating GCV treatment, while GFP>WT mice (n = 5) were not repopulated. (B and C) Infiltrating myeloid cells were more numerous in GFP>TK mice (n = 5 short term, n = 5 long term) than in GFP>WT controls (n = 10), resulting in a higher cell density than resident microglia. Scale bar: 50 µm. Dashed line with green asterisks for comparing GFP^+ cells. One-way ANOVA with Bonferroni *post hoc* analysis. $^{**}p < 0.01$, $^{***}p < 0.001$

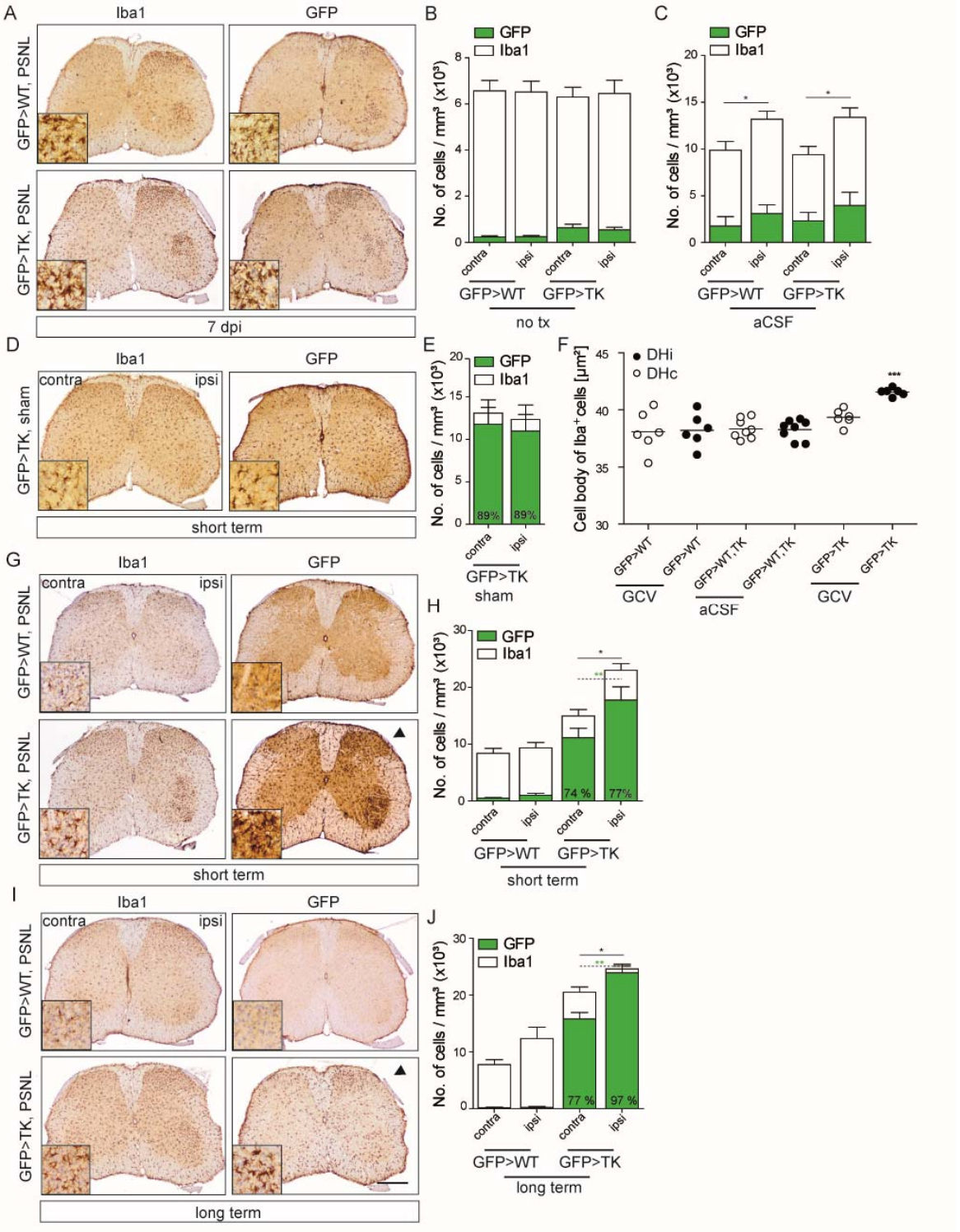
A
Iba1
GFP
GFP>WT, PSNL
GFP>TK, PSNL
7 dpi
B
GFP
Iba1
No. of cells / mm³ (x10³)
contra
ipsi
GFP>WT
GFP>TK
no tx
C
aCSF
D
GFP>TK, sham
short term
E
89%
sham
F
DHi
DHc
Cell body of Iba⁺ cells [µm²]
GCV
aCSF
G
H
74 %
77%
I
long term
J
77 %
97 %

Figure 4. Protracted peripheral myeloid cell reactivity after PSNL in GFP>TK animals. (A) A marked increase in Iba1 and GFP-IR in the lumbar spinal cord in GFP>WT and GFP>TK animals was observed in the ipsilateral dorsal and ventral horn at 7 dpi. (B) Stereological analysis of $Iba1^+$ and GFP^+ cells in the DHi (ipsi) or DHc (contra) revealed no difference in the number of $Iba1^+$ or GFP^+ cells in non-treated GFP>WT (n = 6) and GFP>TK (n = 4) mice. (C) aCSF-treated GFP>WT (n = 7) and GFP>TK (n = 8) mice showed only little infiltration of peripheral myeloid cells, but a significantly higher number of $Iba1^+$ cells within the DHi at 50 dpi, suggesting long-term survival of microglia that proliferated early after PSNL. (D and E) 89% repopulated cells in both the DHi and DHc were observed in sham-operated GFP>TK (n = 5) mice at 50 dpi. (F) Infiltrating myeloid cells in the DHi of GCV-treated GFP>TK mice displayed significantly larger cell bodies (combined short term and long term repopulation groups). (G) $Iba1^+$ and GFP^+ cells in lumbar spinal cord sections at 50 dpi revealed increased numbers of GFP^+ myeloid cells in GFP>TK animals only. Peripheral GFP^+ cells still exhibited morphological signs of activation in the DHi (arrowhead), which could not be found in GFP>WT animals. (H) Stereological analysis of mice shown in (G) revealed a significantly higher number of GFP^+ engrafted myeloid cells in the DHi in repopulated GFP>TK mice (n = 8), but not in their GFP>WT littermates (n = 9). (I and J) A significantly higher number of GFP^+ engrafted myeloid cells was observed in the DHi of long term repopulated mice (n = 5/genotype). Scale bar: 500 µm. Insets were taken from DHi. Error bars represent SEM. Paired two-tailed student´s t-test for corresponding DHc and DHi pairs except for (F), where one-way ANOVA, Bonferroni *post hoc* analysis was used *$p < 0.05$, **$p < 0.01$, ***$p < 0.001$

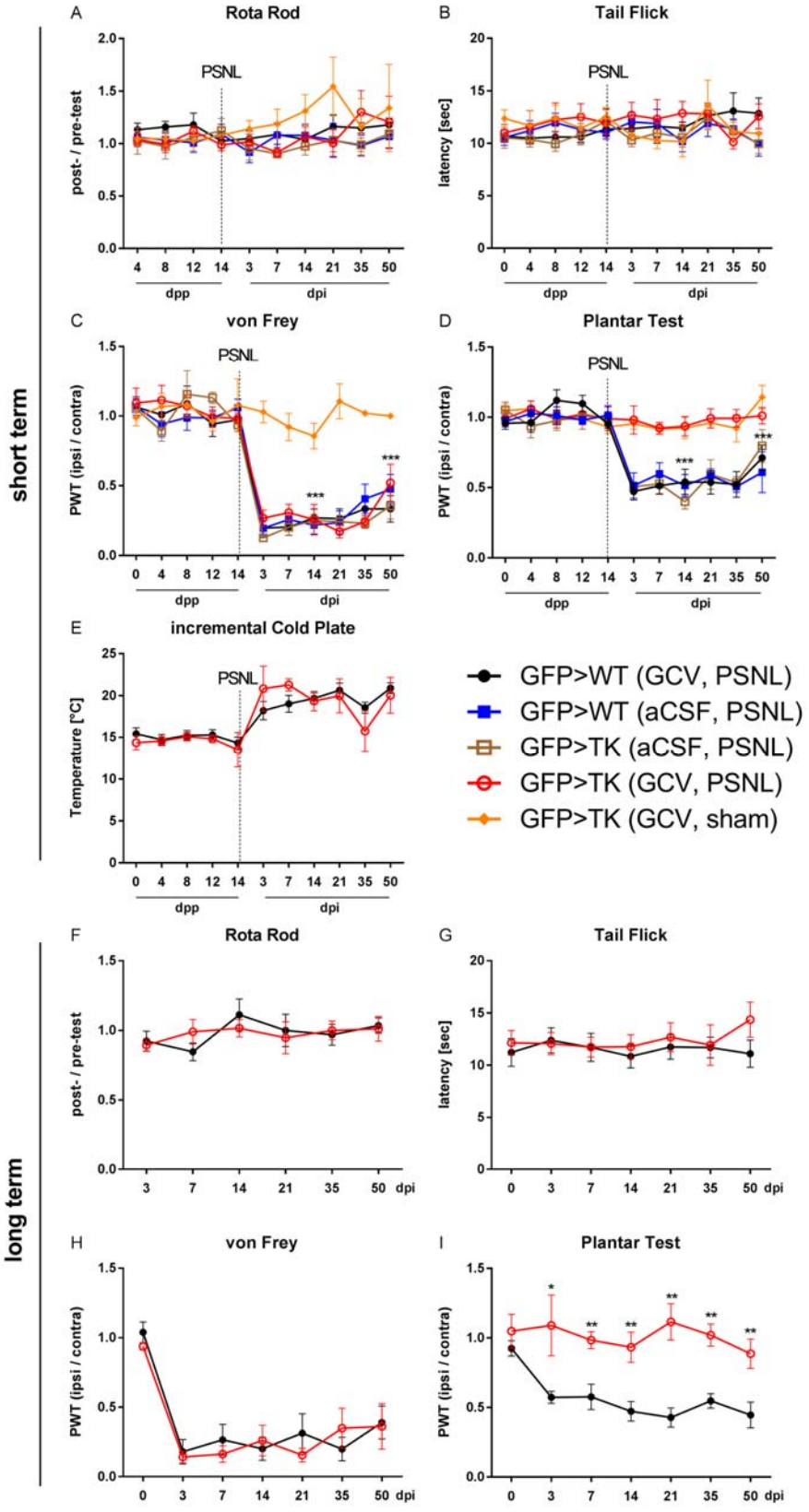
short term
long term
A
Rota Rod
post- / pre-test
PSNL
dpp
dpi
B
Tail Flick
latency [sec]
C
von Frey
PWT (ipsi / contra)
D
Plantar Test
E
incremental Cold Plate
Temperature [°C]
F
G
H
I
GFP>WT (GCV, PSNL)
GFP>WT (aCSF, PSNL)
GFP>TK (aCSF, PSNL)
GFP>TK (GCV, PSNL)
GFP>TK (GCV, sham)

Figure 5. Microglia-depleted mice lack heat hyperalgesia. (A and B) No deficits in the Rota Rod or Tail Flick test could be observed in GCV- or aCSF-treated GFP>WT or GFP>TK animals, as well as in GFP>TK sham-operated controls at several days post pump (dpp) implantation up to 50 days post PSNL. (C-D) No change in baseline values could be observed before PSNL. Manifestation of mechanical allodynia and heat hyperalgesia was detectable in GCV-treated GFP>WT (n = 8), aCSF-treated GFP>WT (n = 8) and aCSF-treated GFP>TK (n = 8) animals after PSNL. In GCV-treated GFP>TK mice (n = 8 up to 21dpi, n = 6 for 35/50dpi), PSNL resulted in a lasting formation of mechanical allodynia, but not heat hyperalgesia. Sham-operated GFP>TK mice (n = 8 up to 7dpi, n = 5-6 for 14/21dpi, n = 2-4 for 35/50dpi) developed neither mechanical allodynia, nor heat hyperalgesia. (E) Increased sensitivity to cold stimuli was only detected after PSNL in GFP>WT (n = 9) and GFP>TK (n = 7 up to 8 dpp, n = 4-6 from 12 dpp onwards) mice. (F and G) At long term repopulation time points, no deficits in the Rota Rod or Tail Flick test were observed in GFP>WT and GFP>TK mice. (H and I) GCV-treated GFP>TK long term repopulated mice (n = 5/genotype) lacked heat hyperalgesia, but developed a lasting mechanical allodynia. Error bars represent SEM. Linear mixed models with adjustment for multiple testing was performed. In *post hoc* tests group differences at 14 and 50 dpi after PSNL were tested. Adjustment for multiple testing was done within each model using Bonferroni correction (A-D). Significant differences for GCV-treated GFP>WT, aCSF-treated GFP>WT, aCSF-treated GFP>TK and GCV-treated GFP>TK mice versus sham-treated mice (C and D). Two-tailed paired student´s t-test (E-I). *$p < 0.05$, **$p < 0.01$, ***$p < 0.001$.

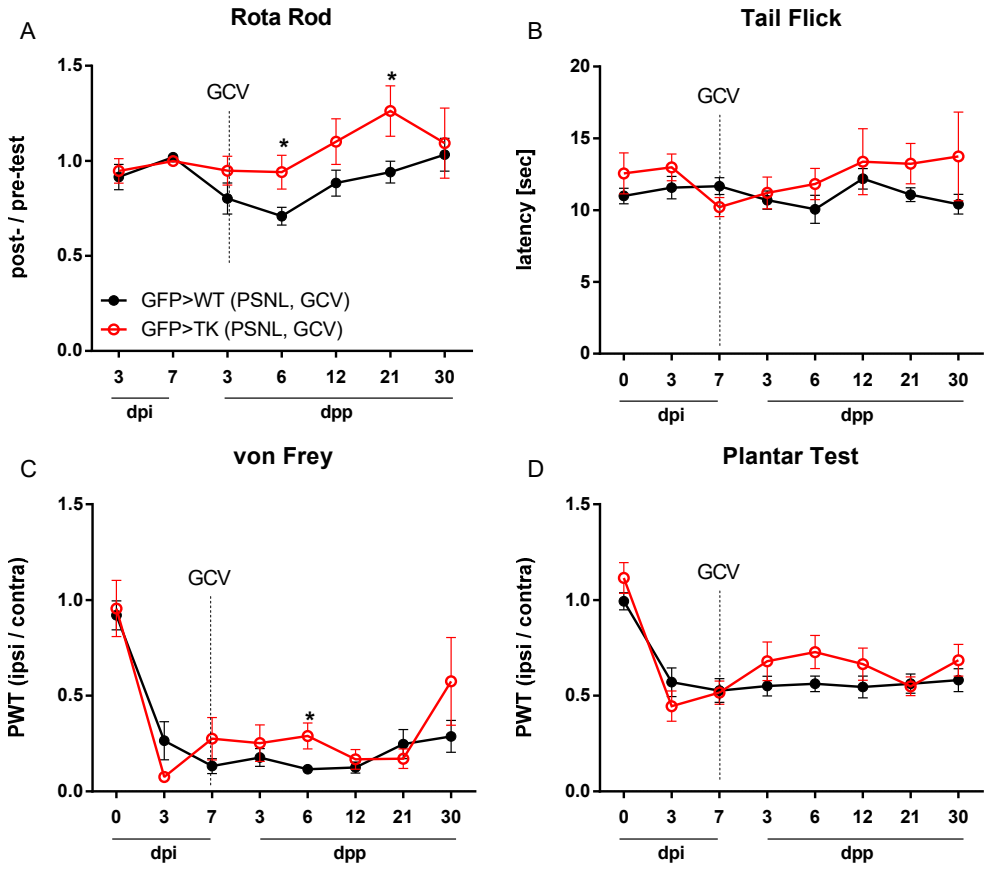

Figure 6: No effect of post-injury microglia depletion and myeloid cell repopulation on existing heat hyperalgesia and mechanical allodynia. (A) Comparable Rota Rod performance between GCV-treated GFP>TK and GFP> WT mice, with the exception of improved performance on 6 and 21 dpp. (B) GFP>WT and GFP>TK mice showed no deficits in Tail Flick testing. (C, D) GFP>WT (n = 7) and GFP>TK (n = 5, n = 3-4 for 21 and 30 dpp) mice developed mechanical allodynia and thermal hyperalgesia after PSNL. These neuropathic pain symptoms were not influenced by microglia depletion and myeloid cell repopulation in both genotypes. Error bars represent SEM. Paired two-tailed student´s *t*-test. *p < 0.05

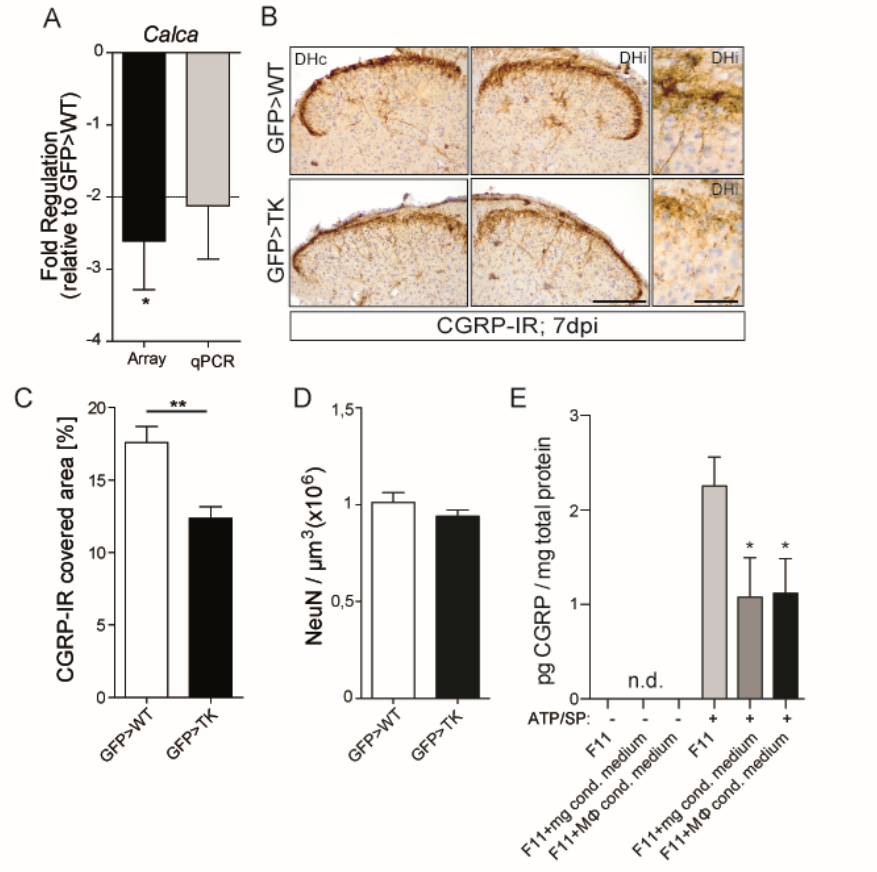

Figure 7. Reduced CGRP expression in the dorsal spinal cord of GFP>TK animals. (A) Differentially expressed *Calca* in GFP>TK relative to GFP>WT mice in array (n = 4/genotype) and by qPCR (n = 3-4/genotype) analyses. Data were normalized to *Gapdh* levels. (B) Central termination of sensory neurons. Representative images of CGRP-IR in cross sections of the lumbar dorsal spinal cord at 7 dpi in GFP>WT and GFP>TK mice. Scale bar: 500 µm, Scale bar magnification: 50 µm. (C) Quantitative morphometric analysis in lamina I of the DH revealed a significantly lower CGRP-covered area in GFP>TK (n = 5) mice, compared to GFP>WT (n = 6) littermates. (D) Quantification of the number of $NeuN^+$ neurons within the lumbar spinal cord of GFP>WT (n = 6) and GFP>TK (n = 4) mice revealed no differences. (E) F11 DRG cells treated with conditioned medium derived from microglia or from peritoneal macrophages (technical triplicates) showed reduced CGRP protein release compared to those that were treated with fresh medium alone. In the absence of ATP and substance P (SP), CGRP was not detectable (n.d.). Error bars represent SEM. (C-D) Paired two-tailed student´s t-test. (E) One-way ANOVA, Bonferroni *post hoc* analysis. *p<0.05, **p<0.01

Table 1: Experimental groups depicting all experimental procedures

Figure	Mice	BMC	icv treatment	PSNL	after PSNL	After 1st manipulation
1A-F	WT	-	-	yes or sham	2 to 90 dpi	0 to 13 wks
1G	WT	X	-	yes	7 dpi	9 wks
2A	TK	X	GCV	yes	50 dpi	17 wks
2B	WT & TK	X	GCV	-	-	10 wk
2C, 4G-H	WT & TK	X	GCV	yes	50 dpi	17 wks
2D, 4C	WT & TK	X	aCSF	yes	50 dpi	17 wks
2E, 4B	WT & TK	X	-	-	-	8 wks
3A-B, 4I-J, 5F-I	WT & TK	X	GCV	yes	50 dpi	31 wks
3C	WT & TK	X	GCV	yes	50 dpi	17 & 31 wks
4A, 7A-E	WT & TK	X	GCV	yes	7 dpi	11 wks
4D-E	WT	X	GCV	sham	50 dpi	17 wks
4F	WT & TK	X	GCV or aCSF	yes	50 dpi	17 & 31 wks
5A-E	WT & TK	X	GCV or aCSF	yes or sham	50 dpi	17 wks
6A-D	WT & TK	X	GCV	yes	37 dpi	13 wks

aCSF: artificial cerebrospinal fluid, BMC: bone marrow chimeras, dpi: days post injury, GCV: Ganciclovir, icv: intracerebroventricular, PSNL: partial sciatic nerve ligation, TK: *CD11b-HSVTK* mice, wks: weeks, WT: wild type mice